Supersonic Aerodynamics of Spinning Tubular Bodies

E. Politis* and R. J. Kind†
Carleton University, Ottawa, Canada

Two distinct flow regimes are possible for spinning tubular projectiles (STUP's) moving at supersonic speeds: a low-drag "started" regime and a high-drag regime in which the flow inside the STUP is choked. This makes STUP's attractive for use in gunnery practice. Relatively simple, computationally fast methods have been synthesized for predicting the aerodynamic characteristics of STUP's. The flow is considered to consist of a number of subfields, namely, external and internal inviscid, leading edge, base, and boundary layers. For each of these, analysis methods are outlined for both the started and choked flow regimes. Theoretical methods from the literature are used with appropriate empirical modifications where necessary. Where comparison with experimental data for STUP's is possible, agreement is generally good. Observed STUP trajectories agree well with those calculated using predicted aerodynamic characteristics.

I. Introduction

TWO quite different flow regimes can occur for a tubular projectile in supersonic flight. At relatively low supersonic Mach numbers, the flow inside the tube (the internal flow) is choked, and a detached bow shock occurs upstream of the projectile, as sketched in Fig. 1a. At relatively high Mach numbers the internal flow is "started," and an attached shock- and expansion-wave system prevails as sketched in Fig. 1b. In choked flow, much of the shock system is normal, or nearly normal, to the freestream direction, and large entropy and static-pressure increases thus occur. Consequently, the drag force is relatively high in choked flow as compared to started flow.

Because of these phenomena, tubular projectiles are attractive for use as practice rounds for tank gunnery. The projectile normally leaves the tank-gun's muzzle at about Mach 4.5 and the started flow regime prevails; the projectile gradually decelerates and, at some point along its trajectory, the flow switches to the choked regime. By suitable design the switch to choked flow can be made to occur shortly beyond the gun-to-target distance, which is normally much less than the total trajectory length for tank-gun projectiles. Thus, the trajectory of the tubular practice round can be tailored to match that of the actual round over the gun-to-target distance, while the remainder of the trajectory is substantially shortened due to the switch to the high-drag choked flow regime. This offers the potential for large reductions in land area devoted to gunnery ranges, an important consideration, particularly in Europe.

Tubular projectiles are also potentially attractive as ammunition for low-level strafing runs since they are less likely to ricochet into the path of the aircraft.

The projectiles are normally spin-stabilized; hence the term spinning tubular projectiles (STUP's). Canada's Department of National Defence and Canadian Arsenals Ltd. have been developing STUP's for some years.

For design purposes, methods were required for predicting aerodynamic coefficients of STUP's as functions of Mach number, angle of attack, and STUP geometry. This paper outlines the methods synthesized for these purposes. The aerodynamic coefficients include axial and normal force, pitching moment, Magnus force and moment, and roll and pitch damping. Mach number and angle of attack ranges are $1.5 \leq M_\infty \leq 5$ and $-10 \text{ deg} \leq \alpha \leq 10 \text{ deg}$, respectively. The STUP geometry is assumed to be as shown in Fig. 2. Three leading-edge configurations are considered; namely, sharp, rounded, and blunt wedge, designated types A, B, and C, respectively (see Fig. 2). Geometric parameters are assumed to have values within the ranges listed in Fig. 2.

A comprehensive set of wind-tunnel data was available for three STUP configurations, designated A, B, and C in accordance with their leading-edge types.[1,2] Table 1 lists the configuration parameters of these three STUP's. These data comprised detailed pressure surveys over the external and internal surfaces of a sting-mounted STUP for Mach numbers and angle of attack up to 4.0 and 10 deg, respectively. The wind-tunnel model was not spinning but Reynolds numbers were representative of flight conditions.

To formulate prediction methods, the overall flowfield was considered to consist of a number of subfields and regimes, and these were modeled using relatively simple theoretical methods available in the existing literature. In some cases, the theoretical models were adjusted to bring them into agreement with the available experimental data. Wherever possible, the prediction methods were validated against the experimental data. The resulting computer code enables rapid and inexpensive prediction of the aerodynamic coefficients required for trajectory analysis for STUP's. Computational fluid dynamics (CFD) techniques are sufficiently advanced that finite-difference solution of the Euler or Navier-Stokes equations could be contemplated for STUP configurations. However, computer codes based on this approach would not have been sufficiently rapid or cost-effective for extensive use in preliminary design studies.

II. Aerodynamic Prediction Methods

A. Overview

The overall force and moment coefficients for any particular STUP configuration are considered as the sum of contributions from the following flowfields: leading edge, external inviscid, internal inviscid, base, and viscous boundary layers. Each of these flowfields must be analyzed for both started and choked flow. In addition, the starting and choking Mach numbers must be predicted for any given STUP configuration. The methods adopted for these purposes are outlined in the following subsections. Comparisons with experiment are also shown. Additional details are given in Ref. 2.

Submitted Oct. 18, 1985; presented as Paper 86-0395 at the AIAA 24th Aerospace Sciences Meeting, Reno, NV, Jan. 6-9, 1986; revision received June 7, 1986.

*Research Associate, Department of Mechanical and Aeronautical Engineering; presently at Engine Laboratory, National Research Council, Ottawa, Canada.

†Professor, Department of Mechanical and Aeronautical Engineering. Member AIAA.

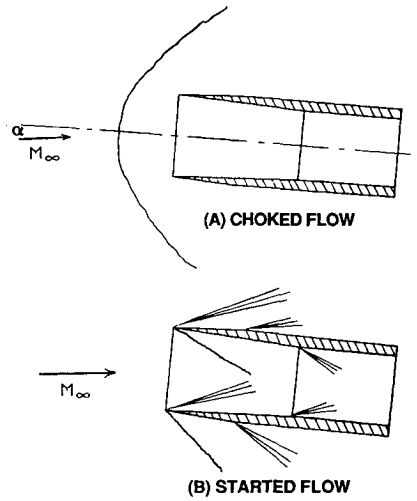

Fig. 1 Choked and started flow regimes.

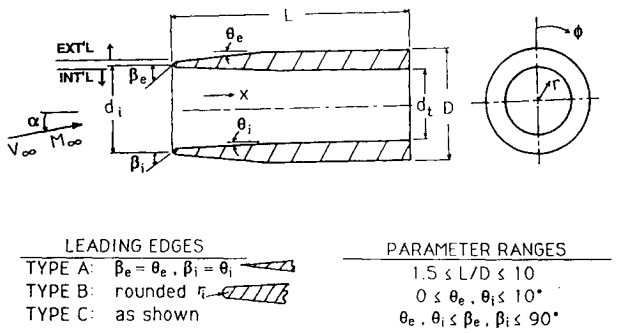

Fig. 2 STUP configurations.

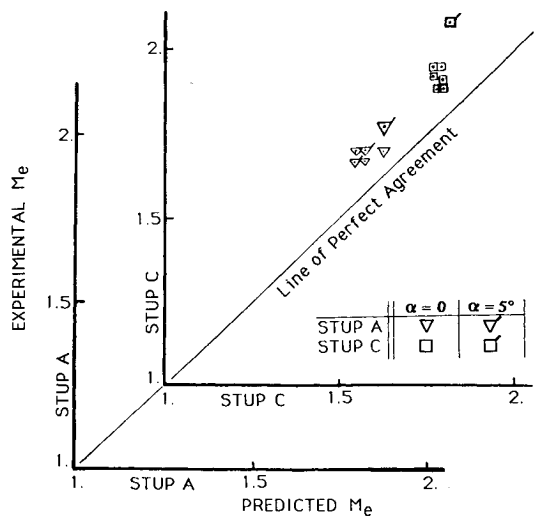

Fig. 3 Comparison of predicted and experimental shock-expulsion Mach numbers.

B. Starting and Choking

The starting of a STUP is identical to the well-known problem of the starting of a fixed-geometry supersonic engine inlet.[3] The minimum Mach number at which a STUP will start is that at which the throat can just pass the entire mass flow in the steam tube bounded by the inlet circle (diameter d_i) with a plane normal shock at the leading edge. The bow shock is then "swallowed," giving the started flow regime of Fig. 1b. Normal-shock and one-dimensional isentropic flow theory are used to relate the minimum starting Mach number to the area ratio $(d_t/d_i)^2$. If the muzzle-exit Mach number exceeds the minimum starting value, the bow shock is swallowed suddenly. The internal flow is then similar to that in a shock tube just after rupture of the diaphragm, and it can be argued that there cannot be any significant boundary layer at the shock to affect the swallowing process. Boundary-layer displacement effects are therefore neglected. Unfortunately, no suitable experimental results are available for comparison with the analysis.

One-dimensional isentropic flow theory is also used to determine the freestream Mach number at which the flow will switch to the choked regime. The freestream Mach number M_∞ is assumed to prevail over the inlet plane; the Mach number at the throat, M_t, is a function of M_∞ and of the area ratio $(d_t/d_i)^2$, as established by the one-dimensional theory. As M_∞ decreases, M_t approaches unity and choking occurs. The throat is no longer able to pass all the mass flow "captured" by the inlet, the shock system is expelled, and the choked flow regime of Fig. 1a is established. In this case, a boundary-layer displacement correction is appropriate. A simple, two-dimensional, turbulent boundary-layer correlation[4] is used to determine an effective throat area for use in the theory. The method gives shock-expulsion Mach numbers that agree well with experimental value deduced from Figs. 19-24 of Ref. 5 for a variety of STUP's (see Fig. 3).

C. External Inviscid Flow

A linear theory for the external and internal supersonic flow past a tube of nearly constant radius at small incidence has been developed by Lighthill[6] and Ward.[7,8] The theory is based on the linearized potential equation for supersonic flow and assumes that the leading edge of the tube is sharp so that the bow waves are attached and the external and internal flows are independent. It yields simple expressions for the drag, lift, and moment coefficients, involving only the angle of attack, slope of the meridional section at any point, and certain auxiliary functions W and V. The latter are the same for all tube shapes and are functions only of the nondimensional parameter $z = x/\beta r_m$; x, β and r_m are, respectively, the axial coordinate, $\sqrt{M_\infty^2 - 1}$, and an appropriate mean radius. W and V are made up of modified Bessel functions and represent the solution of the linearized potential equation for the pressure perturbations due to tube cross-section shape and incidence, respectively. Appropriate integration of W gives the axial force; integrations of V give the normal force and pitching moment. The functions are tabulated in Refs. 7 and 9 and, in the present work, were curve-fitted with high-order polynomials in z. This greatly facilitates the necessary integrations over tube length.

This theory was used for determining the contribution of the external inviscid flow to the coefficients of axial and nor-

Table 1 Configuration parameters of tested STUP's

Designation	L, mm	D, mm	d_i, mm	d_t, mm	Θ_e, deg	Θ_i, deg	r_i, mm	β_e, deg	β_i, deg
A	262.5	105	95.76	80.14	3	3	—	3	3
B	237.1	105	95.76	80.14	3	3	1.4	—	—
C	315.0	105	88.39	80.14	3	3	—	34	3

mal force, pitching moment and pitch damping on STUP's with both sharp and blunt leading edges and for both started and choked flow. For started flow, no modifications to the theory were necessary although, in the case of blunt leading edges, additional contributions to the aerodynamic coefficients were introduced using a leading-edge flow model (outlined in Subsec. IIE). The origin for x is placed at the start of the mildly sloped (slope θ_e) conical portion of the forebody. With choked flow, the external and internal flows are not independent, and use of Ward's theory is not strictly valid. However, it was considered that the spillage of flow around the inlet lip would not dramatically alter the external flow pattern and forces on the STUP. Consequently, the theory, with some empirical modifications, was also used for choked flow.

For the external flow analysis, the mean radius r_m, which appears in the parameter z, is set equal to an x-weighted mean radius of the external (see Fig. 2) contour of the STUP. The mean is for the entire external contour except in the case of axial force, when it is for the conical forebody only. For configurations of the type shown in Fig. 2, only the conical forebody (slope θ_e) contributes to the wave drag; the axial force is taken as the wave drag at zero angle of attack. The normal force and pitching moment are independent of the tube shape and are proportional to angle of attack for this theory.

The pitch damping is obtained on the basis of the assumption that the flow in any given cross-flow plane is independent of that in adjacent planes and that the pitch rate q produces an effective incidence (qx^1/V_∞) where x^1 is the distance from the center of gravity. The pitch-damping coefficient can then be expressed in terms of an integral of $(\partial L(z)/\partial z)$, where $L(z)$ is an integral of the auxiliary function V and is itself a function of z only. $L(z)$ represents the lift or normal force distribution along the body.

For choked flow, the calculation of external axial force contribution is not modified. There is no theoretical justification for this, but this contribution is only about 2% of the total axial force for the choked flow regime, so great accuracy is not essential.

For choked flow, the theoretical function $L(z)$ is replaced by a modified function, $L(z)_c$, which is curve-fit to the experimental data for external lift contribution vs z for choked flow conditions. The contributions to normal force, pitching moment, and pitch damping are calculated in the usual way, using this $L(z)_c$. r_m is set to 0.5 D. $L(z)_c$ is reliable only up to $z \leq 4$, since there are no experimental data for higher z.

Figure 4 shows some comparisons between calculated and experimental results for the external inviscid flow for three STUP configurations. The steps in the calculated curves correspond to the shock-expulsion Mach number. The agreement is reasonably good except for C_A at low Mach numbers and, as already mentioned, this is unimportant because this contribution to C_A is then only about 2% of the total.

D. Internal Inviscid Flow

The internal flow is considered to comprise all the flow inside the STUP. The internal inviscid flow is analyzed quite differently for started and choked flow. In the case of blunt leading edges, the force and moment contributions are supplemented by contributions from a leading-edge flow model.

The internal flow does not contribute significantly to pitch damping. This is because the mass of fluid inside the STUP at any instant is relatively small and the angular momentum changes it incurs solely as a result of pitch rate are negligible.

Started Flow

Except for Ward's[7,8] linear theory, which applies only for $z<2$ in internal flow, no complete theoretical solution has been found to the complex problem of supersonic flow inside a cylindrical tube. A periodic "diamond" wave pattern, with nondimensional cell length $\Delta z \cong 2$, tends to occur near the tube inlet, but the wave interactions are not regular (Mach disks occur), and Ferri[10] has shown that the flow may become subsonic at the tube centerline. The periodicity of the flow is attenuated with increasing z and, for $z>5$, slender body theory can be used.[11] Thus, theoretical solutions are available for $z<2$ and for $z>5$, while empirical correlations must be used in between.

The approach used for started internal flow was entirely similar to that used for the external flow, Subsec. IIC; that is, the auxiliary functions were fitted by polynomials in z, and the necessary integrations were performed to obtain the force and moment contributions.

Only the conical forebody (slope θ_i) contributes to the axial force and, in practice, z is less than 2 for this portion of STUP's. Therefore, the theoretical auxiliary functions for the internal flow, tabulated in Ref. 7, were curve-fitted for this purpose. For these calculations, the mean radius r_m in the parameter z was that of the internal conical forebody.

As for the external flow, a function $L(z)$ is required for the normal-force and pitching-moment contributions. For this purpose, a curve-fit to a combination of theoretical and experimental results was used; namely, linear theory results (tabulated in Ref. 9) for $z<2$, experimental data of Roe[9] and Cook[11,12] for $2 \lesssim z \lesssim 5$, and slender body theory for

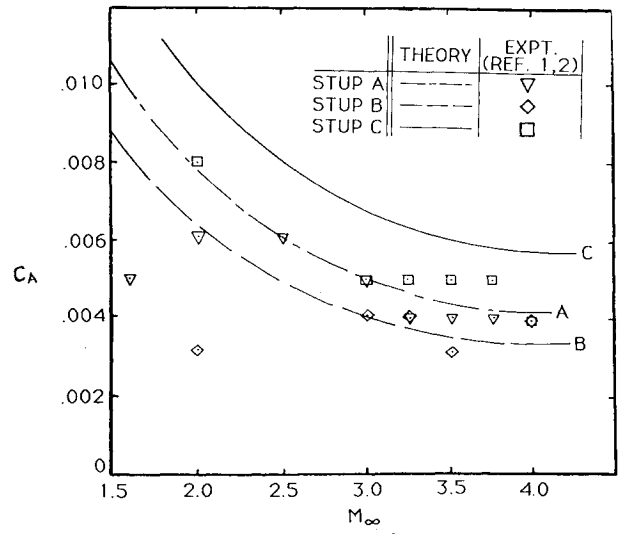

a) Axial pressure force.

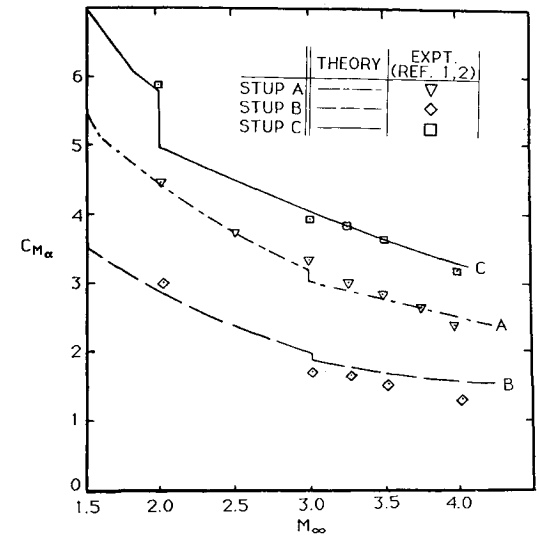

b) Pitching moment derivative.

Fig. 4 Comparison between predicted and experimental axial pressure force and pitching moment results for external flow.

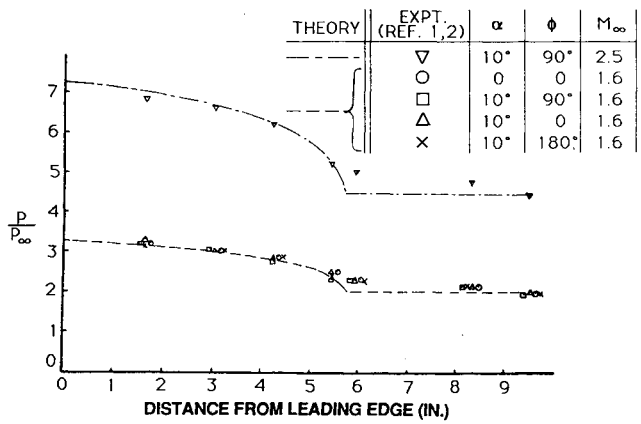

Fig. 5 Theoretical and experimental pressure distributions for internal flow, choked regime.

$z>5$; r_m was set to $d_t/2$ for this function, since this gave the best correlation of the experimental results.

Choked Flow

For the choked regime, the internal flow is well represented by assuming that the fluid has passed through a normal shock and then using one-dimensional isentropic flow theory, with $M=1$ at the throat. Figure 5 shows typical comparisons between calculated and experimental pressure distributions. Note that there is negligible circumferential variation of static pressure within the STUP, implying that the internal flow is in the axial direction, except presumably near the inlet plane.

Axial and normal force can thus be determined by applying the momentum theorem to a control volume that encloses the entire internal flow. No integrations are necessary with this approach. It is assumed that the flow is in the freestream direction where it enters this control volume (at the inlet plane). The data of Fig. 5 imply that the turning to the axial direction takes place quite near the inlet plane, so the normal force can be assumed to act here. The pitching moment is calculated on the basis of this assumption.

Comparisons with Experiment

Figure 6 compares calculated and experimental contributions of the internal flow to the pitching moment derivative for both started and choked flow. The agreement for axial and normal force contributions is at least as good.

E. Leading-Edge Flow

In the case of blunt leading edges, a leading-edge flow model is required to supplement the external and internal flow models. The leading-edge region is considered to comprise the rounded or blunt wedge portion of the STUP section; that is, the portion upstream of the conical forebody of slope θ_e or θ_i. To be useful for present purposes, the leading-edge flow model must be relatively simple and computationally fast. The approximate method of Moeckel[13] was chosen. The ratio of leading-edge thickness to STUP diameter is sufficiently small that the flow can be assumed to be locally two-dimensional at any circumferential position ϕ. Only drag forces are considered; any lift developed at nonzero angle of attack is considered to be included in the external and internal flow models.

Started Flow

Moeckel's method will be outlined with reference to Fig. 7. The detached shock is assumed to be a hyperbola that is asymptotic to the freestream Mach lines. It has been shown that the sonic point *sb* on a rounded body is approximately the point at which the body contour is inclined at the maximum flow turning angle for an oblique shock at the particular freestream Mach number M_∞. The sonic point *s* on the shock is located where the shock angle and M_∞ are such that the oblique shock solution gives a downstream Mach number of unity. The sonic line is assumed to be a straight line joining points *s* and *sb*. Average properties of the fluid crossing the sonic line are assumed to be those prevailing on the centroid streamline ($y=y_s/2$ upstream of shock), with velocity normal to the sonic line. Continuity can then be used to determine the ratio A_s/A_∞ and thus the length of the sonic line. The sonic line is assumed to be inclined at angle η given by $0.5\ (\delta_s+\delta_{max})$, where δ_s and δ_{max} are the flow turning angles at points *s* and *sb*, respectively. Knowing *s*, A_s, and η establishes the position of the shock relative to the body.

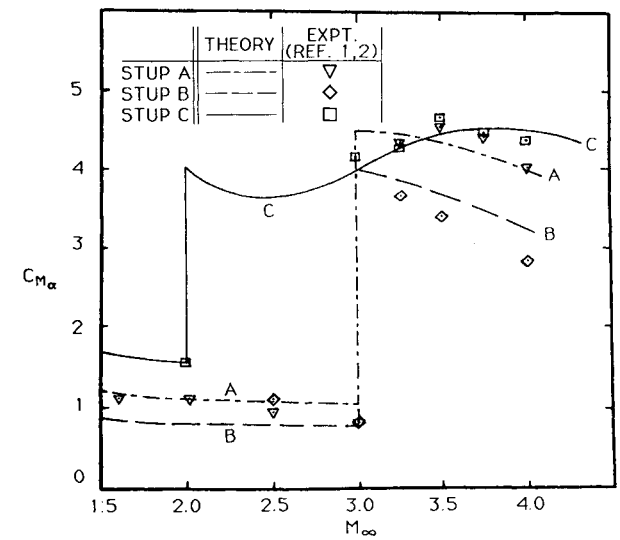

Fig. 6 Comparison between predicted and experimental results for pitching moment contributions of internal flow.

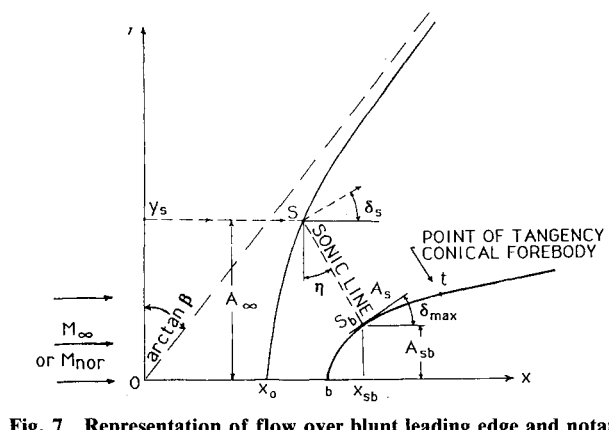

Fig. 7 Representation of flow over blunt leading edge and notation used in the analysis (after Moeckel[13]).

The flow model of the preceding paragraph allows the form drag upstream of the sonic point *sb* to be calculated by application of the momentum theorem to the control volume *O-b-sb-s-*y_s in Fig. 7. The form drag on the remainder of the leading edge, *sb* to *t* in Fig. 7, is obtained by assuming a Prandtl-Meyer expansion along this portion of the body contour. For simplicity, the average pressure is assumed to be the pressure at the midpoint of the arc *sb* to *t*. On the basis of experimental evidence,[14] the pressure ratio P_{sb}/P_∞ at the sonic point is assumed to be that of an isentropic expansion to $M=1$ from conditions downstream of a normal shock at M_∞.

The above description has assumed a rounded leading edge (type B). For a blunt wedge leading edge (type C), the

analysis is very similar, provided the flow turning angle δ imposed by the wedge exceeds δ_{max}, the maximum possible for an oblique shock at M_∞. The body sonic point *sb* is then at the joint between the blunt wedge of slope β_e or β_i and the conical forebody of slope θ_e or θ_i. The external or internal inviscid flow model is applied immediately downstream of point *sb*. If δ is less than δ_{max}, the bow shock is attached and oblique shock theory can be used instead of Moeckel's model to determine the pressure, and thus the form drag, on the leading edge.

Point b in Fig. 7 is assumed to be the most upstream point on the STUP section, and the foregoing analysis is applied separately outside and inside this point. When the angle of attack of the STUP is nonzero, conditions vary circumferentially around the inlet. The analysis is then applied to circumferential segments of arc length $\Delta\phi = 10$ deg. In each segment, the normal component of Mach number, $M_{nor} = M_\infty \cos\alpha/\cos\alpha_{eff}$, is used instead of M_∞, and an effective angle of attack, $\alpha_{eff} = \alpha \cos\phi$, is used. The x axis of Fig. 7 is aligned with the $\alpha_{eff} = 0$ direction; in general, therefore, this axis is not parallel to the centerline of the STUP, and this fact is recognized when flow turning angles imposed by the body contour are computed. The drag forces for all segments $\Delta\phi$ are summed and resolved into contributions to axial and normal force and pitching moment on the STUP.

Choked Flow

Moeckel[13] also extended his model to enable prediction of the additive drag due to spillage for supersonic inlets. Figure 8 shows the flow model. The spillage drag is defined as the integral of axial pressure force along the dividing streamline from *Q* to *sb*.

The present internal model for choked flow (see Subsec. IID) already includes this spillage drag, since the plane *TR* of Fig. 8 serves as the upstream face of the control volume used in that analysis. Thus, the overpressure and flow deceleration associated with spillage are included in the momentum balance used to determine the internal drag force contribution in choked flow cases. Moeckel's model is therefore used only to evaluate the pressure drag on the portion *R-sb* of the leading edge. For this purpose, the momentum equation in applied to control volume *O-T-R-sb-s-Y_s-O* in Fig. 8.

F. Base Flow

Of course, the base pressure makes a significant contribution to the axial force on a STUP. Unfortunately, established base-pressure correlations are only available for two-dimensional or nontubular axisymmetric configurations. Provided that the ratio (d_t/D) is reasonably close to unity, the flow in the base region of a STUP at small angle of attack should be locally two-dimensional. However, the flow is unusual in that the bounding flows (internal and external flows) are not the same. The difference is especially marked in the choked flow regime.

For started flow cases, a correlation similar to Love's[15] was formulated, using Love's two-dimensional data together with data from the STUP wind-tunnel tests.[1,2] The correlation is a polynominal in M_∞, which gives the base-pressure coefficient, shown in Fig. 9. Despite the use of experimental data for STUP's in formulating the correlation, it cannot be considered completely reliable because sting interference effects may have been important in the wind-tunnel tests. The model was supported by four struts (continuations of the STUP section), which covered about one-third the base area and divided the base flow into four cells.

In the case of choked flow, the internal flow at the base is exactly sonic. Fuller and Reid[16] investigated a flow similar to the one existing at the base of a choked STUP. They found that the ratio of internal stagnation pressure to freestream static pressure has a strong influence on the base pressure, since it controls the relative turnings of the two flows as they expand around the shoulders at the base. In the case of choked STUP's, this pressure ratio is a function only of the Mach number M_∞. A polynomial giving the base-pressure coefficient as a function of M_∞ was fitted to the test data for choked STUP's; this correlation is shown in Fig. 10.

For both started and choked STUP's, the experimental base pressures showed little dependence on angle of attack ($\alpha \leq 10$ deg).

G. Viscous Boundary Layers

Typical Reynolds numbers for STUP's are such that transition occurs relatively close to the leading edge. Therefore, it is reasonable to assume turbulent flow over the entire length of the STUP.

Skin-Friction Drag

Hoerner[17] gives a formula that approximates the Schoenherr[18] skin-friction correlation for flat plates; he also gives a Mach number correction for adiabatic-wall conditions. The wetted area of STUP's is used with these relations to estimate the skin-friction drag. The Reynolds and Mach numbers are based on freestream conditions for the external flow and for started internal flow. For choked internal flow, the numbers are based on throat flow properties.

Roll Damping

Since STUP's are spin-stabilized, estimates of spin decay rate are required. For small angles of attack ($\alpha \leq 10$ deg), cross-flow effects on roll-damping torque are expected to be negligible; therefore, only the $\alpha = 0$ case needs to be considered.

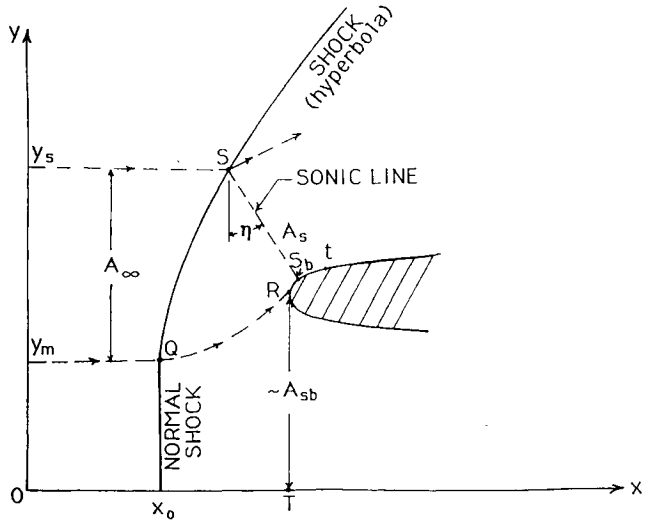

Fig. 8 Representation of flow past supersonic inlet with spillage.

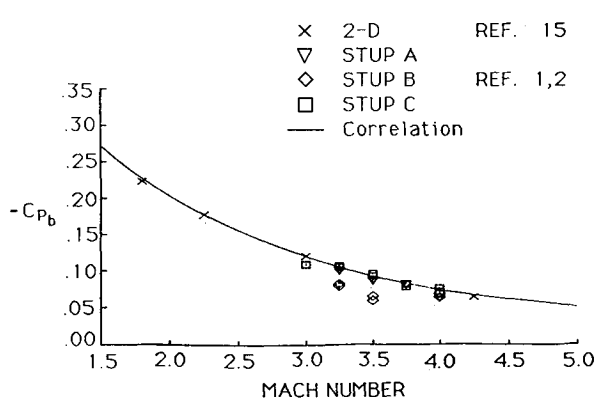

Fig. 9 Base-pressure coefficient, started flow.

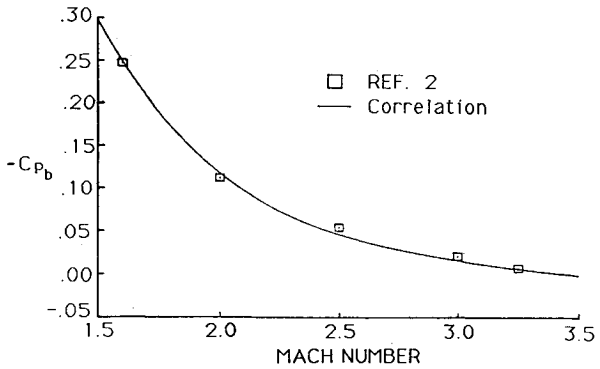

Fig. 10 Base-pressure coefficient, choked flow.

A freestream particle follows a spiral path relative to the surface of the STUP; the helix angle λ is given by arc tan $(pD/2V_\infty)$, where p is the roll or spin rate. Coriolis forces in the relative reference frame act normal to the STUP's surface. Assuming that axial and circumferential pressure gradients are small, there cannot be any skewing of the relative velocity profiles in the boundary layer. Consequently, the boundary layer will be essentially the same as that on a flat plate, with the effective distance from the leading edge being equal to the distance along the spiral particle paths and the resultant wall shear stress acting at angle λ to the axial direction.

For typical STUP applications, $\cos\lambda \cong 1$, and the resultant wall shear stress is nearly equal to the axial shear stress component, and $\sin\lambda$ is approximately equal to the nondimensional roll rate. The roll-damping torque is then $(D/2 \sin\lambda)$ times the axial friction force of the preceding subsection, and the roll-damping coefficient is thus equal to 0.5 times the axial friction-force coefficient, a result also obtained by Charters and Kent.[19]

Magnus Effects

When STUP's are at angle of attack, the cross flow is not symmetric because of the effects of spin on the viscous flow in the boundary layer. This gives rise to a side force (i.e., force normal to the plane of the angle of attack) and yawing moment on the STUP.

Jacobson[20] and Platou[21] have reviewed work on Magnus effects. These are known to be highly variable functions of the boundary layer, the nose and base shapes, and discontinuities in streamline shape; moreover, angle of attack, fineness ratio, spin rate, and Reynolds and Mach numbers are important. While small compared to the normal force, the Magnus force can significantly affect the flight trajectory of a slender projectile.

The method of Vaughn and Reis[22] was selected because it gives simple closed-form solutions and is easily adapted for open-nosed bodies such as STUP's. Also, the method includes the effect of the radial pressure gradient in the boundary layer, which is ignored by most other investigators, as well as the effect of leeside vortices, which is accounted for by an empirical relation obtained from wind-tunnel tests. Vaughn and Reis[22] showed good agreement with data[21,23] for unfinned bodies of revolution at supersonic Mach numbers.

In his discussion of the method of Ref. 22, Jacobson[20] points out the sensitivity of Magnus effects to transition location. In the present case, this presents no difficulties, because unit Reynolds numbers of STUP's are of order 5×10^7/m and transition occurs within about 30 mm of the leading edge. It is therefore adequate to assume fully turbulent flow, at least for 105-mm-diam STUP's.

Only the external flow over the STUP is assumed to give rise to Magnus effects. This is based on the assumption that the internal flow will always be essentially axial, on average, so that there is no cross flow to give rise to asymmetries and Magnus effects.

Details of the method as applied to STUP's are given in Ref. 2.

III. Discussion

Simplicity was an essential requirement for the methods to predict aerodynamic characteristics of STUP's. The methods that have been outlined meet this requirement although, of course, this sometimes involves some compromise with exactness.

Wherever possible, the prediction methods were validated against experimental data, and agreement in such cases was generally good. Several of the prediction methods, however, (e.g., external flow for the choked regime and base flow) made use of curve-fits to the only data available for STUP's,[1,2] and truly independent validation was not possible. Furthermore, no suitable data were available for individual validation of some of the other flow models, including the leading-edge and viscous flow analysis. Nevertheless, the methods appear to give good overall predictions of STUP aerodynamics, because STUP trajectories calculated using the aerodynamic prediction code, together with a six-degree-of-freedom trajectory code, agree well with observed trajectories.[24] Experience[24] indicates that the present methodology is quite satisfactory for purposes of preliminary design.

IV. Conclusions

The aerodynamic characteristics of STUP's can be predicted using relatively simple methods.

It is expedient to break down the overall flow into a number of subfields, namely, external inviscid, internal inviscid, leading-edge, base, and boundary layers. Separate analysis methods were formulated for each of these, for both the started and the choked flow regimes.

It was possible to base the analyses on existing methods, but empirical modifications were required in several cases.

Where comparison with experimental data for STUP's was possible, agreement was generally good. Lack of suitable data, however, prevents comprehensive validation of the prediction methods.

Observed STUP trajectories agree well with those calculated using aerodynamic characteristics predicted by the present methods.

Acknowledgment

This work was carried out under a research contract awarded on behalf of the Department of National Defence of Canada, Defence Research Establishment Valcartier.

References

[1]Atraghji, E., "Internal and External Surface-Pressure Measurements on Three SRC Tubular Configurations in the Mach Number Range 0.8-4.0," National Research Council of Canada, Rept. NAE-LTR-HA-5X5/0104, Sept. 1978.

[2]Politis, E., Kind, R. J., and Abdel-Hamid, A. N., "An Aero Prediction Method for Tubular Shapes at Supersonic Mach Numbers," Carleton University Centre for Advanced Engineering and Design, Ottawa, Ontario, Canada, Final Rept., Vol. 1, Sept. 1983.

[3]Shapiro, A. H., *The Dynamics and Thermo-dynamics of Compressible Fluid Flow,* Ronald Press, New York, Vol. 1, 1953, pp. 149-154.

[4]Schlichting, H., *Boundary Layer Theory,* 4th ed., McGraw-Hill, New York, 1960, pp. 536-537.

[5]Atraghji, E., "An Experimental Investigation to Study Shock-Expulsion and Shock Swallowing on the 105 mm STUP," National Research Council of Canada, Rept. NAE-LTR-HA-5X5/0109, April 1977.

[6]Lighthill, M. J., "Supersonic Flow Past Bodies of Revolution," ARC RM 2003, Jan. 1945.

[7]Ward, G. N., "The Approximate External and Internal Flow Past a Quasi-Cylindrical Tube Moving at Supersonic Speeds," *Quarterly Journal of Mechanics and Applied Mathematics,* Vol. 1, June 1948, pp. 225-245.

[8]Ward, G. N., *Linearized Theory of Steady High Speed Flow,* Cambridge University Press, Cambridge, England, 1955, pp. 167-182.

[9]Roe, P. L., "An Experimental Investigation of the Flow Through Inclined Circular Tubes at a Mach Number of 4.0," RAE TR 65110, May 1965.

[10]Ferri, A., "Application of the Method of Characteristics to Supersonic Rotational Flow," NACA TN-1135, 1946.

[11]Cook, P. H., "Supersonic Wind Tunnel Measurements of the Loads and Internal Pressure Distributions on Internally Parallel Ducts at Incidence," RAE TN Aero. 2962, May 1964.

[12]Cook, P. H., "Supersonic Wind Tunnel Measurements of the Loads and Internal Pressure Distributions on Ducts at Incidence," RAE TN Aero. 1951, Feb. 1964.

[13]Moeckel, W. E., "Approximate Method for Predicting Form and Location of Detached Shock-Waves Ahead of Plane or Axially Symmetric Bodies," NACA TN-1921, July 1949.

[14]D'Souza, N., Molder, S., and Moretti, G., "Numerical Method for Hypersonic Internal Flow Over Blunt Leading Edges and Two Blunt Bodies," *AIAA Journal,* Vol. 10, May 1972, pp. 617-622.

[15]Love, E. S., "The Base Pressure at Supersonic Speeds on Two-Dimensional Airfoils and Bodies of Revolution (with and without Fins) Having Turbulent Boundary Layers," NACA RM L53CO2, April 1953.

[16]Fuller, L. and Reid, J., "Experiments on Two-Dimensional Base Flow at M=2.4," R.A.E. Rept. Aero. 2569, Feb. 1956.

[17]Hoerner, S. F., *Fluid-Dynamic Drag,* published by the author, 2 King Lane, Greenbriar, Brick Town, NJ, 1965, pp. 2-5.

[18]Schoenherr, K. E., "Resistance of Plates," *Transactions of the Society of Naval Architects and Marine Engineers,* Vol. 40, 1932, pp. 279-313.

[19]Charters, A. C. and Kent, R. H., "The Relation Between the Skin Friction Drag and the Spin Reducing Torque," BRL Rept. 287, U.S. Army Ballistic Research Laboratory/ARRADCOM Aberdeen Proving Ground, MD, 1942.

[20]Jacobson, I. D., "Magnus Characteristics of Arbitrary Rotating Bodies," AGARD-AG-171, Nov. 1973.

[21]Platou, A. S., "Magnus Characteristics of Finned and Non-finned Projectiles," *AIAA Journal,* Vol. 3, Jan. 1965, pp. 83-90.

[22]Vaughn, H. R. and Reis, G. E., "A Magnus Theory for Bodies of Revolution," Sandia National Laboratories, Rept. SC-RR-72 0537, Albuquerque, NM, Jan. 1973.

[23]Luchuk, W., "The Dependence of the Magnus Force and Moment on the Nose Shape of Cylindrical Bodies of Fineness Ratio 5 at a Mach Number of 1.75," NAVORD Rept. 4425, White Oak, MD, April 1957.

[24]D'Souza, N., private communication, Canadian Arsenals Ltd., Montreal, Quebec, Canada, 1984.